Pion-Nucleon Scattering in the Boundary Condition Model. II. The Second Resonance*†

H. GOLDBERG‡ AND E. L. LOMON
Department of Physics and Laboratory for Nuclear Science, Massachusetts Institute of Technology, Cambridge, Massachusetts

(Received 25 October 1963; revised manuscript received 15 January 1964)

Good agreement is obtained with experimental information on the second pion-nucleon resonance by considering an explicit coupling to the ρ-nucleon channel. The dynamics are represented by the boundary-condition model, satisfying analytic and unitarity requirements. The main effect is due to the coupling to virtual ρ mesons, in contrast to the S-state coupling effects. All the isotopic splitting of the $J=\frac{3}{2}$ D states can be explained by the coupling to the ρ-nucleon channel. By altering the coupling in accordance with the one-pion exchange diagram the $T=\frac{3}{2}$ 850-MeV "shoulder" is obtained. The boundary-condition radius agrees with the relevant Feynman diagrams of the strip approximation.

I. INTRODUCTION

THE introduction of inelastic unitarity to the problem of the scattering of two particles has been attempted by several authors in several different dynamical schemes for both π-N[1–4] and $\bar{K}$-N[5] scattering. In most cases the hope has been that the unitarity conditions combined with reasonable causality and dynamical assumptions (analyticity, zero-range boundary conditions, etc.) would be sufficient to introduce a maximum in the (π-N or $\bar{K}$-N) cross section. In previous work[6,7] we have explored the effects on S-wave π-N scattering of including production channels in the unitarity dynamical approximation of the boundary-condition model. This scheme assumes independent homogeneous boundary conditions on the various two-particle-channel wave functions at a boundary radius suggested by a consideration of the dominantly contributing diagrams. The results in the S-wave case have been in good agreement with experiment from 0–700 MeV and have explained the isotopic splitting of the $T=\frac{1}{2}$ and $T=\frac{3}{2}$ waves at threshold. In the S-wave case, the 2 pions in the inelastic channel are considered to be strongly correlated in the $T=0$, $J=0^+$ state at a low kinetic energy in their c.m. In that case the second channel causes strong energy dependence mainly above its threshold. In this paper we shall apply the unitary model to the problem of the second resonance of the π-N system. Here we shall demonstrate that a resonance may be produced in the $T=\frac{1}{2}$, $J=\frac{3}{2}$ D state far below the threshold of the second channel, casting doubt on the validity of using elastic unitarity for low-energy calculations.[7] Even then energies above inelastic threshold are of such importance to the dispersion integrals as to bring in inelastic unitarity in an important way.

It is shown that, as in the S states,[7] all the isotopic splitting of the $J=\frac{3}{2}$ D states can be attributed to the difference in coupling to the ρ-nucleon intermediate state. If the ratio of the couplings is taken to be the same as that of the one-pion exchange graphs, the $T=\frac{3}{2}$, $J=\frac{3}{2}$ D state is compatible with experiment, including the $T=\frac{3}{2}$, 850-MeV "shoulder."

II. THE SECOND RESONANCE

General Considerations

The first observed maximum in the π-N total cross section occurs at $T_\pi=190$ MeV (where $T_\pi=$ lab kinetic energy of the pion). It has been known for some time, with little ambiguity, that this is essentially an elastic "dynamic" resonance in which the P_{33} phase shift goes through 90° at the cross-section maximum with negligible absorption. The force due to the exchange of a nucleon supplemented by the requirement of a right-hand unitary cut in the amplitude including the rescattering is adequate to predict a resonance in this state.[8]

However, when we come to the second maximum at $T_\pi=600$ MeV, no such clear situation exists. From experiment we know that the maximum occurs not only in the total $T=\frac{1}{2}$ cross section, but also separately in the $T=\frac{1}{2}$ elastic and inelastic cross sections at this energy.[9–11] No amplitude analysis yet points definitely

* Supported in part through funds provided by the Atomic Energy Commission under Contract At(30-1)-2098.

† Based in part on a thesis submitted by one of us (H. G.) to the Department of Physics, MIT, in partial fulfillment of the requirements for the Ph.D. degree.

‡ Present address: Department of Physics, Brandeis University, Waltham, Massachusetts.

[1] P. Carruthers, Ann. Phys. (N.Y.) **14**, 229 (1961).

[2] J. S. Ball and W. R. Frazer, Phys. Rev. Letters **7**, 204 (1962).

[3] J. S. Ball, W. R. Frazer, and M. Nauenberg, Phys. Rev. **128**, 478 (1962).

[4] L. F. Cook, Jr. and B. W. Lee, Phys. Rev. **127**, 283, 297 (1962).

[5] R. Dalitz, Phys. Rev. Letters **6**, 239 (1961).

[6] H. Goldberg and E. L. Lomon, Phys. Rev. **131**, 1290 (1963). Hereafter referred to as G.L.

[7] H. Goldberg and E. L. Lomon, Phys. Letters **8**, 368 (1964).

[8] G. F. Chew, M. L. Goldberger, F. E. Low, and Y. Nambu, Phys. Rev. **106**, 1337 (1957).

[9] J. A. Helland, T. J. Devlin, D. E. Hagge, H. J. Lango, B. J. Moyer, and C. D. Wood, Phys. Rev. Letters **10**, 27 (1963).

[10] T. J. Devlin, B. J. Moyer, and V. Perez-Mendez, Phys. Rev. **125**, 690 (1962).

[11] P. Falk-Vairant and G. Valladas, *Proceedings of the Tenth Annual International Conference on High Energy Physics at Rochester* (Interscience Publishers, Inc., New York, 1960).

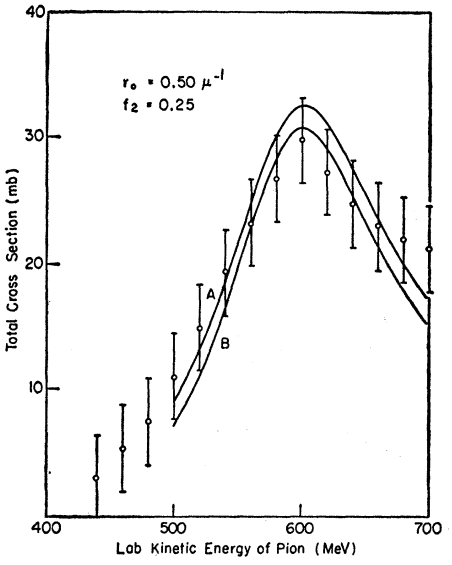

(a)

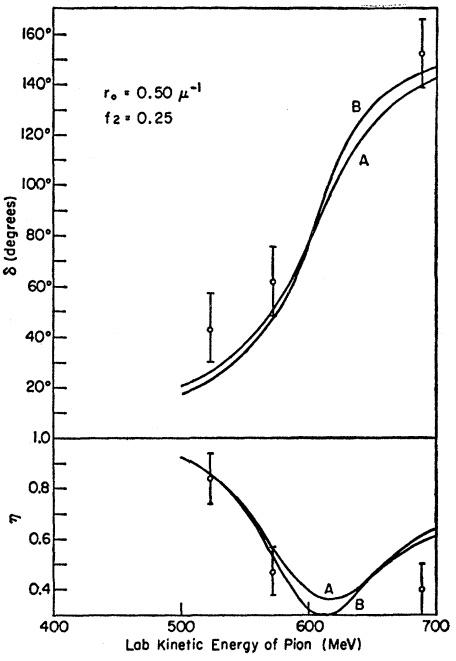

(b)

FIG. 1. The total D_{13} cross section ["(a)" part of figure] and δ, η ["(b)" part] obtained from the coupled-channel B.C.M. equations as derived in Sec. 4 with $r_0 = 0.50\,\mu^{-1}$. The experimental points are from Ref. 10 with 30 ± 1 mb subtracted as nonresonant background. Parameters for the various curves are found in Table I.

to any particular partial wave as being responsible for these maxima although the assumption that the D_{13} state goes through resonance is consistent with all results.

Most attempts to explain the maximum require that the singularities (forces) responsible for inelastic events also give rise to an elastic maximum at the same time, the general driving agent being inelastic intermediate states acting through unitarity in the physical channel. Thus it is very important to maintain unitarity while

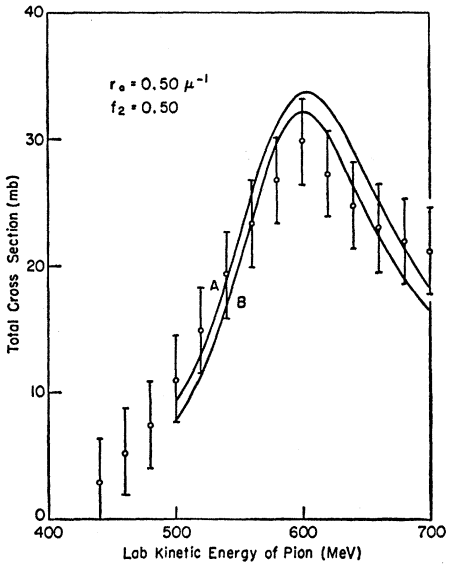

(a)

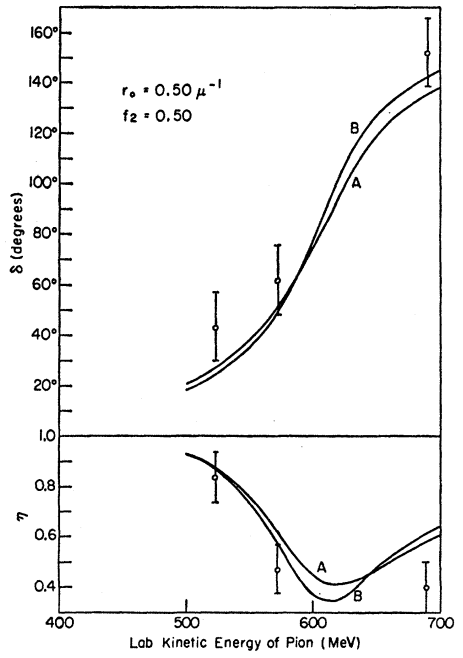

(b)

FIG. 2. The total D_{13} cross section ["(a)" part of figure] and δ, η ["(b)" part] obtained from the coupled-channel B.C.M. equations as derived in Sec. 4 with $r_0 = 0.50\,\mu^{-1}$. The experimental points are from Ref. 10 with 30 ± 1 mb subtracted as nonresonant background. Parameters for the various curves are found in Table I.

prescribing the forces to be used. Ball, Frazer, and Nauenberg[3] point out in detail the difficulties involved in doing this. In G.L. we saw how by using the unitary coupling forces generated by the simple boundary-condition model (B.C.M.) we could generate amplitudes which have the correct general nature, and whose particular character depends on the π-π interaction. As pointed out in the discussion in Ref. 7, the elastic amplitude in the S_{11} case was driven mostly by "ABC" pairs on the mass shell, and thus the major rise in cross section came *above* threshold. In the case of D_{13} waves (the component most suspect in forming the second resonance), Cook and Lee[4] have inferred that the major contribution to the amplitude comes from dispersion over ρ's produced virtually while Ball and Frazer[2] conjecture that on-the-mass-shell production contributed from the low-energy tail of the ρ is sufficient to give the second resonance. The purpose of this paper is to show that the unitary forces generated by the B.C.M can produce a resonance *below* threshold due solely to virtual intermediate state effects, and thus unify the two points of view within a single framework. This will now be done using much of the formulation in G.L.

Experimental Data

Most of the data we use for comparison with our results is from experiments done at Berkeley.[9,10] At present more of these are being conducted (such as $\pi^-+p\rightarrow\pi^0+n$ differential cross sections), eventually enabling one to make a more definite amplitude analysis. In this section we shall describe some of the results of the aforementioned experiments and the conclusions that can be drawn from them.

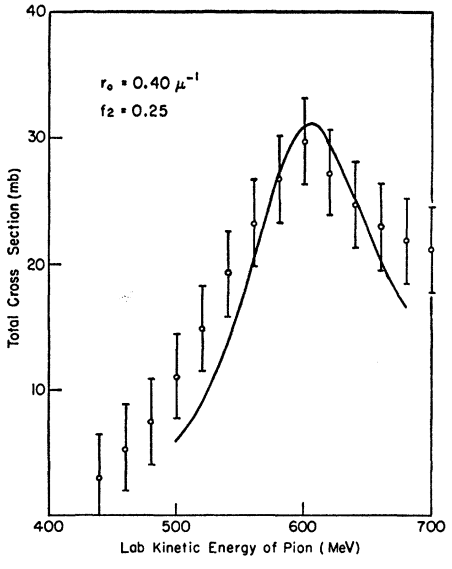

FIG. 3. Total D_{13} cross sections for $r_0=0.40\,\mu^{-1}$, $f_2=0.25$. Parameters in Table I.

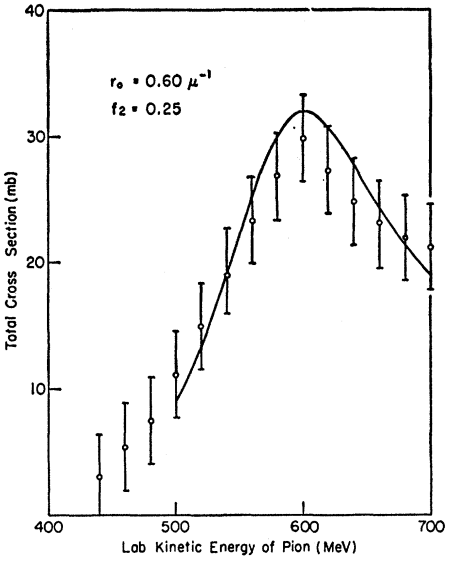

FIG. 4. Same as 3 for $r_0=0.60\,\mu^{-1}$, $f_2=0.25$.

(a) *Total Cross Section*

By considering the isotopic composition of the incoming states, one may derive the formulas

$$\sigma_{\rm tot}(\tfrac{1}{2})=\tfrac{3}{2}\sigma_{\rm tot}(\pi^-p)-\tfrac{1}{2}\sigma_{\rm tot}(\pi^+p)\,,$$
$$\sigma_{\rm tot}(\tfrac{3}{2})=\sigma_{\rm tot}(\pi^+p)\,. \qquad (2.1)$$

Using the total cross sections given in Ref. 10, together with the experimental errors given there, we calculate $\sigma_{\rm tot}(\frac{1}{2})$. Subtracting 30 ± 1 mb as nonresonant background, we obtain the points shown in comparison to the curves in Figs. 1(a), 2(a), 3, and 4. The errors which were within 10% of each other, have been rounded off to an average ±3.3 mb over the range of the measurements. The background subtraction of 30 mb is obtained from the background between resonances over the range 0.5–1.5 BeV.[10] The error may in fact be larger than ±1 mb.

We now wish to inquire whether this maximum in the scattering cross section at 600 MeV arises from a resonance in a single state of total angular momentum J and orbital angular momentum l.

The total and elastic cross sections for such a state (for given isospin) are given by

$$\sigma_{\rm tot}(l,J)=(4\pi/k^2)(J+\tfrac{1}{2})\,{\rm Im}A_{lJ}\,, \qquad (2.2)$$
$$\sigma_{el}(l,J)=(4\pi/k^2)(J+\tfrac{1}{2})\,|A_{lJ}|^2\,, \qquad (2.3)$$

where

$$A_{lJ}=\frac{\eta_{lJ}e^{2i\delta_{lJ}}-1}{2i}\,, \qquad (2.4)$$

k is the c.m. momentum, and $0\leq\eta_{lJ}\leq1$. At resonance ($\delta_{lJ}=\pi/2$),

$$\sigma_{\rm tot}^{\rm (res)}=(4\pi/k_{\rm res}^2)(J+\tfrac{1}{2})[\tfrac{1}{2}(1+\eta_{lJ})]. \qquad (2.5)$$

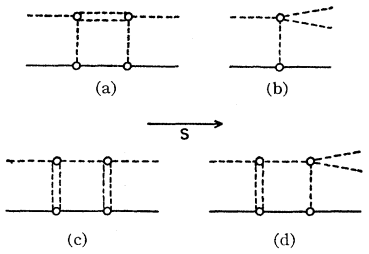

FIG. 5. (a), (b): Graphs contributing to potential-type elastic scattering and production, respectively. (c), (d): Graphs contributing to B.C.M.-type elastic scattering and production, respectively.

Thus

$$\frac{2\pi}{k^2}\leq\frac{\sigma_{\text{tot}}}{(J+\frac{1}{2})}\leq\frac{4\pi}{k^2}. \tag{2.6}$$

In general, k^2 is given by

$$k^2=\frac{2MT_\pi(2MT_\pi+4M\mu)}{4[2MT_\pi+(M+\mu)^2]}. \tag{2.7}$$

For $(T_\pi)_{\text{res}}=600$ MeV$=4.34\,\mu$ and $M=6.80\,\mu$, we obtain

$$k_{\text{res}}{}^2=10.8\,\mu^2$$
$$=0.53\ \text{mb}^{-1}.$$

Therefore,

$$12\ \text{mb}\leq\frac{\sigma_{\text{tot}}}{J+\frac{1}{2}}\leq 24\ \text{mb}. \tag{2.8}$$

From Fig. 6(a)

$$\sigma_{\text{tot}}{}^{(\text{res})}\approx 30\ \text{mb}. \tag{2.9}$$

Thus we find from (2.8) and (2.9) that all J's but $J=\frac{3}{2}$ are inconsistent with experiment. The η required for $J=\frac{3}{2}$ leads to $(\sigma_{el}/\sigma_{\text{tot}})=0.64$. This considerable inelasticity is verified by the experiments of Ref. 11.

The analysis of photoproduction experiments by Peierls[12] indicates $l=2$ for this resonance. If this is so, then the channel responsible for the resonance is D_{13} if we accept the above reasoning. The P_{13} possibility (also employed in Ref. 13) has not yet been definitely eliminated by any analysis (although in the analysis of Roper[14] it is discouraged, even in combination with a D_{13} resonance).

(b) *Other Data*

Fitting the total $\pi^{\pm}p$ cross sections, differential cross sections for the processes $\pi^+ + p\rightarrow\pi^+ + p$ and $\pi^- + p\rightarrow\pi^- + p$, polarization measurement and using the forward dispersion relations, Eandi[13] has obtained a set of "nonunique but plausible" *SPD* amplitudes, assuming that the D_{13} phase shift goes through 90° in the vicinity of 600 MeV. The phase shift δ and the inelastic parameter η for D_{13} scattering are given as the experimental points in Figs. 1(b) and 2(b) as a function of T_π. The allowable variation of the amplitude fit was not discussed in the above reference. By considering the experimental accuracy of the differential cross section and of the inelasticity[15] we arrived at the error bars shown in the figures.

Another recent analysis,[14] fitting directly to data with energy-dependent amplitudes, shows much the same behavior of the D_{13} amplitude in this energy range if a D_{13} resonance is assumed.

So we shall proceed on the assumption that the D_{13} channel is of paramount importance in the scattering. This choice will be seen to be compatible with our model.

III. INELASTIC CHANNELS

Again as in G.L. we introduce a production channel

$$\pi+N\rightarrow\pi+\pi+N$$

in which we must decide, as in the S-wave case, how to correlate two of the three particles in the final state. We may once more try a π^* of $T=0$, $J=0^+$. But we are now 400 MeV above the threshold for the main contribution from such a process, and it can probably be safely discounted as a strong structural effect, although some further exploration is warranted.

According to the latest analyses[16] the quantum numbers of the η meson are $J^{PG}=0^{-+}$, where P denotes parity and G denotes the eigenvalue of the G-parity operator $Ce^{i\pi(T_2+\frac{1}{2}Y)}$.[17] This assignment also fits in neatly with the "eight-fold way."[18] The J^P assignment of 0^- prohibits any $\eta\rightarrow 2\pi$ vertex, while $\eta\rightarrow 3\pi$ is allowed only through a violation of $\Delta G=0$, since the G parity of 3 pions is negative. Thus the η is eliminated from consideration in any peripheral production process such as Figs. 5(b), (d).

ρ versus $N_{33}{}^*$

Now we shall give arguments for considering the coupling of the two pions into $T=1$, $J=1$ (ρ meson) as of more importance than the coupling of one of the pions and the nucleon into $T=\frac{3}{2}$, $J=\frac{3}{2}^+$ (N^*).

(a) Let us picture the nucleon as consisting of a pion ($T=1$) bound to a core ($T=\frac{1}{2}$) in a p state so

[12] R. F. Peierls, Phys. Rev. **118**, 325 (1960).
[13] R. Eandi, University of California, Lawrence Radiation Laboratory Report No. UCRL-10629 (unpublished)
[14] L. D. Roper, private communication and Ph.D. thesis, Massachusetts Institute of Technology (unpublished); Phys. Rev. Letters **12**, 340 (1964).
[15] H. Goldberg, Ph.D. thesis, Massachusetts Institute of Technology, 1963 (unpublished).
[16] P. L. Bastein, J. P. Berge, O. I. Dahl, M. Ferro-Luzzi, D. H. Miller, *et al.*, Phys. Rev. Letters **8**, 114 (1962); M. Chretien, F. Bulos, H. R. Crouch, Jr., R. E. Lanou, Jr., J. T. Massimo, *et al.*, *ibid.* **9**, 127 (1962).
[17] P. Roman, *Theory of Elementary Particles* (North-Holland Publishing Company, Amsterdam, 1960).
[18] M. Gell-Mann, Phys. Rev. **125**, 1067 (1962). The η is there referred to as χ_0.

that the isotopic spin of this system (the physical nucleon) is $\frac{1}{2}$.[19] The incoming pion has $T=1$.

If the production is mainly $\rho+N$, we expect Fig. 6(a) to be representative of the process. Here the exchanged pion is the bound pion in our model of the physical nucleon.

If, however, $\pi+N^*$ dominates the production channel, then Fig. 6(b) will presumably play a major role in the process. The exchanged nucleon in this diagram is the bare nucleon of our model, while the outgoing pion is the bound pion which has been released by the scattering.

Since the resonance occurs in the state of *total* $T=\frac{1}{2}$ with no special activity in the $T=\frac{3}{2}$ channel at these energies, there would be support for that process which gives a larger ratio of $T=\frac{1}{2}$ to $T=\frac{3}{2}$. The coupling of three isotopic spins with one pair in a definite state t'' can be represented by

$$\Psi(t''T;T_z)=\sum_{t'} R(t_1t_2t_3T;t't'')\Phi(t'T;t_z), \quad (3.1)$$

where R is a unitary matrix symmetric in t' and t'', and can be chosen real. Φ is a state with particles 1 and 2 coupled to isospin t', whereas Ψ has particles 2 and 3 coupled to t''. Independent of all magnetic quantum numbers, R is related to the 6-j symbol through the relation

$$R(t_1t_2t_3T;t't'')=(-1)^{t_1+t_2+t_3+T}[(2t'+1)(2t''+1)]^{1/2} \times\begin{Bmatrix} t_1 & t_2 & t' \\ t_3 & T & t'' \end{Bmatrix}. \quad (3.2)$$

For process 6(a): $t_1=\frac{1}{2}$ (the bare nucleon); $t_2=1$ (the bound pion); $t_3=1$ (the incoming pion); $t'=\frac{1}{2}$ (the physical nucleon); $t''=1$ (the ρ meson). Hence from the known values of the 6-j symbol[20] the ratio of probabilities is

$$\frac{(T=\frac{1}{2})}{(T=\frac{3}{2})}=\frac{4}{1}. \quad (3.3)$$

On the other hand, we have for N^* production through process 6(b): $t_1=1$ (the bound pion); $t_2=\frac{1}{2}$ (the bare nucleon); $t_3=1$ (the incoming pion); $t'=\frac{1}{2}$ (the physical nucleon); $t''=\frac{3}{2}$ (the N^*). The resulting ratio in this case is

$$\frac{(T=\frac{1}{2})}{(T=\frac{3}{2})}=\frac{8}{5}. \quad (3.4)$$

Thus we find that the ρ mechanism, Fig. 6(a), favors $T=\frac{1}{2}$ production much more than the N^* process, Fig. 6(b), if indeed these diagrams dominate the mechanisms.

[19] J. Hamilton and T. D. Spearman, Ann. Phys. (N. Y.) **12**, 172 (1961).

[20] M. Rotenberg, R. Bivins, N. Metropolis, and J. K. Wooten Jr., *The 3-j and 6-j Symbols* (Technology Press, Cambridge, Massachusetts, 1959).

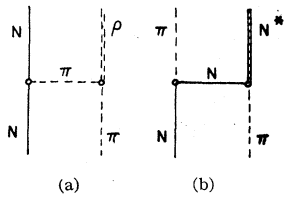

FIG. 6. (a) Peripheral production of ρ meson: Model discussed in text has exchanged pion coupled to nucleon core (in exit channel) in P_{11} state. (b) Short-range N^* production: Here the exchanged nucleon is core bound to pion (in exit channel) in P_{11} state.

(b) The model of the physical nucleon proposed in (a), in which a pion is bound to a nucleon core in a P_{11} state, has some other interesting consequences concerning the total energies of the lab π-bound π and lab π-bare N systems in their respective centers of mass. From the relation $kr\sim l$, when the angular momentum barrier is overcome, we find for the p state ($l=1$) that for $r\sim 1\,\mu^{-1}$ (one-pion exchange), we have $k\sim\mu=140$ MeV/c for the average magnitude of the momentum of the bound pion (or bare nucleon), in the lab system.

From this very crude assumption one may deduce[15] that at 600 MeV the average energy in the π-π center of mass is down about 3 half-widths from the peak of the ρ, while the average energy in the incoming π-exchanged N center of mass is up about 6 half-widths from N^* energy. Thus again we favor the ρ meson.

(c) From the invariance property of $E^2-\mathbf{P}^2$ where $E=$total energy, $\mathbf{P}=$total momentum, we find that the threshold lab kinetic energy for the creation of mass m in the c.m. system in π-N scattering is given by

$$(T_\pi)_{\rm thr}=\frac{m^2-(M+\mu)^2}{2M}. \quad (3.5)$$

If we take the ρ as a zero-width particle of mass 5.21 μ, we find

$$(T_\pi)_{\rm thr}=6.13\mu=846\ \text{MeV}. \quad (3.6)$$

For an N^* of mass 8.96 μ

$$(T_\pi)_{\rm thr}=389\ \text{MeV}. \quad (3.7)$$

The first of these is up 150 from $T_\pi=600$ MeV, the second is down 210 MeV. In the case of the ρ we shall demonstrate the strong influence of producing ρ's virtually at energies far below threshold. We have seen, however, that in the case of the ABC, which has its influence mainly through the Ball-Frazer effect of producing particles on the mass shell, the major effects appear at or slightly above threshold. Thus, at least in our model, the N^* mechanism (whose effects would be of the ABC or Ball-Frazer genre) would probably play little part at 600 MeV.

(d) The fact that the resonance is probably $l=2$ suggests that the long-range peripheral model [Fig. 6(a)] dominates rather than the very short-range nucleon exchange force [Fig. 6(b)] or other multipion exchange diagrams which could lead to an N_{33}^*.

(e) The isobar-production model agrees quite well with the $Q(N,\pi)[=(E_{N\pi}{}^2-\mathbf{P}_{N\pi}{}^2)^{1/2}-(M+\mu)]$ values

found in the reactions $\pi^+ + p \to \pi^+ + \pi^0 + p$ and $\pi^+ + p \to \pi^+ + \pi^+ + n$, but is not very convincing in the $\pi^- + p \to 2\pi + N$ values.[21] The results in this latter case suggest the dominance of the ρ meson.

However, in spite of all these arguments, there can be no doubt that, even if the primary mechanism is the peripheral production of the ρ meson, the final-state rescattering of one of the pions and the nucleons through the (3.3) isobar will be of great importance in predicting the Q values of the final-state particles. The coupling of the N^* into the problem is feasible in this model and will be attempted in future work. Meanwhile, we adopt ρ-N as the inelastic channel of primary importance.

The ρ-N, S-state channel presumably also couples strongly to the $T=\frac{1}{2}$, $J=\frac{1}{2}$ and $\frac{3}{2}$ P-state π-N channels. Because of the importance of the pole term and short-range exchange potential in these states we do not treat them in the present context. Furthermore it is possible to use crossing properties to relate the even and odd angular momentum π-N states. Work is now in progress using these connections.

IV. DETAILS OF THE MODEL AND THE FITTING OF THE DATA

Here we proceed in much the same way as in the S_{11} case of G.L.

The Boundary Condition

Let the reduced radial wave functions in the π-N channel be $u(W,r)$, where W is the total energy in the π-N c.m. system. If the reduced radial wave function in the ρ-N system is $w(m,W,r)$ for a ρ meson of mass m, then the dynamical B.C.M. equations are

$$\begin{aligned} r_0(du/dr)_{r=r_0} &= f_1 u(r_0) + \textstyle\sum_m f_c(m) w(m,r_0), \\ r_0(dw/dr)_{r=r_0} &= f_c(m) u(r_0) + f_2 w(m,r_0). \end{aligned} \tag{4.1}$$

We attempt to allow for the short lifetime of the ρ meson by coupling to channels of varying ρ mass. Here f_1, f_c, and f_2 are real and independent of W. Note the approximation made in neglecting (1) the coupling of various ρ-N channels to each other and (2) the variation of f_2 with m.

By conservation of angular momentum and parity, if the incoming state is D_{13}, the outgoing ρ-N state can have $L=0$ or 2, where $L=$ the orbital angular momentum in the ρ-N c.m. system. The production cross section $\propto 1-\eta^2$. From the Appendix and an equation for arbitrary L analogous to (4.23) one can show from the properties of the Hankel functions that

$$(1-\eta^2) \propto K^{2L+1}, \tag{4.2}$$

for $K \to 0$ (where K is the outgoing c.m. momentum). This, of course, is a result of assumptions far more general than those of the B.C.M. Thus the small L's will manifest themselves first, and so we shall restrict ourselves to the S-wave production of ρ's. Thus we take as the reduced radial ρ-N wave function for $r \geq r_0$

$$W(m,W,r) = B(m,W) e^{iKr}. \tag{4.3}$$

K is the outgoing momentum in the ρ-N c.m. and is given by

$$K = \frac{[(W^2-(M+m)^2)(W^2-(M-m)^2)]^{1/2}}{2W}, \tag{4.4}$$

where $W=$ total energy in the π-N c.m. and $m=$ mass of the ρ meson produced. W is given in terms of the pion lab kinetic energy T_π by

$$W^2 = 2MT_\pi + (M+\mu)^2. \tag{4.5}$$

For $W<M+m$ (or equivalently $T_\pi < [(M+m)^2 - (M+\mu)^2]/2M$) we are below threshold for production of a mass m meson. Then we let $K \to i\kappa$, and the outgoing (decaying) wave function is given, for $r \geq r_0$, by

$$w(m,W,r) = B(m,W) e^{-\kappa r}, \tag{4.6}$$

where

$$\kappa = \frac{[((M+m)^2-W^2)(W^2-(M-m)^2)]^{1/2}}{2W}. \tag{4.7}$$

We must be very careful in using this formula, since when m and W are such that $m^2-W^2>M^2$, (4.7) predicts *decreasing* binding with *increasing* m for a given W. Even worse, at $m-W>M$, κ again becomes imaginary. A definition of κ which has the required properties for such conditions and which is consistent with a 2-body Klein-Gordon equation (neglecting relative time dependence) has been worked out, but in this paper the values of m^2-W^2 entering the computation will always be less than M^2, and we do not consider this effect which is related to the anomalous threshold.

Thus, using the coupled B.C.M. equations (4.1), and carrying through the calculations with the above wave function w letting $\sum_m f_c(m) \to \int_{2\mu}^{\infty} dm\rho(m)$, we obtain

$$r_0\left(\frac{du}{dr}\right)_{r=r_0} = \left[f_1 + \int_{2\mu}^{\infty} dm\rho(m)\left(\frac{1}{ix-f_2}\right)\right] u(r_0), \tag{4.8}$$

where $u(r)$ is the π-N D_{13}-state reduced radial wave function and

$$\begin{aligned} x &= Kr_0, \quad W>M+m, \\ x &= i\kappa r_0, \quad W<M+m. \end{aligned}$$

The ρ Function: The $T=1$, $J=1^-$ π-π Interaction

Again, as in the S-wave case, we take $\rho(m)$ proportional to the π-π $T=1$, $J=1^-$ cross section at total energy m in the c.m. system. The unitary elastic π-π partial-wave amplitude is

$$\frac{1}{q\cot\delta_{\pi\pi} - iq},$$

[21] M. Olsson and G. B. Yodh, Phys. Rev. Letters **10**, 353 (1963).

where

$$q = \text{momentum in the } \pi\text{-}\pi \text{ c.m.}$$
$$= \tfrac{1}{2}(m^2-4\mu^2)^{1/2}.$$

The results of the model in the π-N channel are insensitive to the details of the π-π cross section. It is sufficient to have a relativistic form that yields the correct position and width. The use of the following simple model for the amplitude allows us to satisfy those conditions and also gives us an effective value for the $\rho\pi\pi$ coupling constant. However this application of the B.C.M. in no way requires the dominance of Fig. 7 in the two pion interaction.

If one introduces a $\rho\pi\pi$ coupling Lagrangian, one obtains from the nonunitary Born (pole) term[1]

$$q^3 \cot\delta_{\pi\pi} \approx m(m^2-m^{*2})/\gamma,$$

where γ is a constant proportional to the $\rho\pi\pi$ coupling constant and m^* is the position of the resonance. The resultant π-π $T=1$, $J=1^-$ amplitude is

$$\frac{1}{[m(m^2-m^*)^2/\gamma q^2]-iq} = \frac{\gamma q^2/m}{(m^2-m^{*2})-i\gamma(q^3/m)}.$$

$$\therefore \rho(m) = N_{\text{res}} D \frac{(m^2-4\mu^2)^2/m^2}{(m^2-m^{*2})^2+\gamma^2(m^2-4\mu^2)^3/m^2}, \quad (4.9)$$

where

$$N_{\text{res}} = \left[\int_{2\mu}^{\infty} dm \frac{(m^2-4\mu^2)^2/m^2}{(m^2-m^{*2})^2+\gamma^2(m^2-4\mu^2)^3/m^2}\right]^{-1}$$

so that

$$\int_{2\mu}^{\infty} \rho(m)dm = D.$$

γ is related to the full width at half-maximum Γ by the relation

$$\gamma = \frac{m^{*2}}{(m^{*2}-4\mu^2)^{3/2}}\Gamma. \quad (4.10)$$

A curve of $\rho(m)$ versus m for this case is shown in Fig. 8.

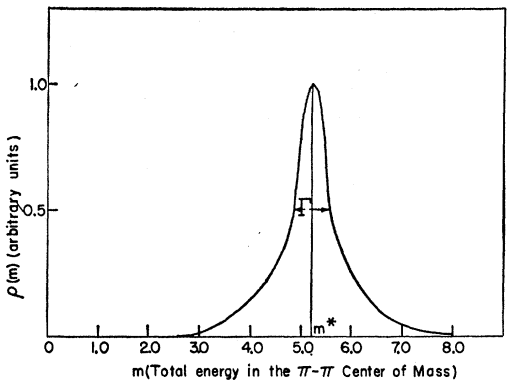

FIG. 8. The function $\rho(m)$ for the $T=1$, $J=1^-$ π-π resonance.

Derivation of the Phase Shift and Inelastic Parameter

Rather than proceeding directly, as in G.L., we shall now outline a method of deriving the amplitude in the most general case (with no potential tail), and from there proceed to give formulas for δ, η, σ, etc., in terms of the amplitude.

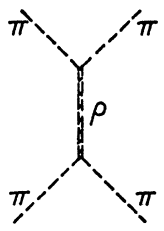

FIG. 7. ρ pole diagram in π-π interaction.

For scattering in any channel (specified by T, J, etc.) the reduced radial wave function is given by

$$u(kr) = \phi^*(kr) + S(k)\phi(kr), \quad (4.11)$$

where the channel subscripts on S and the orbital angular momentum subscript l on ϕ will be henceforth understood. Also the asterisk denotes complex conjugation.

ϕ is the outgoing irregular solution of the reduced radial Schrödinger equation for angular momentum l. We will normalize ϕ so that

$$\phi(z) = z h_l^{(1)}(z), \quad (4.12)$$

where $h_l^{(1)}(z)$ is the outgoing spherical Hankel function of order l. Then

$$\phi(z) = (-i)^{l+1}\chi(z)e^{iz}, \quad (4.12')$$

where $\chi(z)$ is a complex polynomial in z^{-1}, and $\chi \to 1$ as $z \to \infty$.

From the general relationship [e.g., Eq. (4.8)]

$$r_0\left(\frac{du}{dr}\right)_{r=r_0} = f_{\text{eff}}(k^2)u(r_0) \quad (4.13)$$

and (4.11) we obtain the relation between S and f_{eff}

$$S = -\frac{f_{\text{eff}}\phi^* - \beta\phi^{*\prime}}{f_{\text{eff}}\phi - \beta\phi'}, \quad (4.14)$$

where the prime denotes differentiation with respect to $\beta = kr_0$. The partial-wave amplitude is then given by

$$A = (S-1)/2i. \quad (4.15)$$

We now give formulas for the pertinent quantities

in terms of the amplitude A:

(a)

$$\begin{aligned}\eta&=|S|\\&=|1+2iA|\\&=(1+4|A|^2-4\,\mathrm{Im}A)^{1/2},\end{aligned}\tag{4.16}$$

(b)

$$\begin{aligned}\tan\delta&=\left(\frac{1}{-i}\right)\left[\frac{(S/\eta)-1}{(S/\eta)+1}\right]\\&=\left(\frac{1}{-i}\right)\frac{(1-\eta)+2iA}{(1+\eta)+2iA}\\&=\frac{\mathrm{Re}A}{\frac{1}{2}(1+\eta)-\mathrm{Im}A},\end{aligned}\tag{4.17}$$

using the relation (4.16).

(c) The elastic and total cross sections for π-N scattering in a state of definite T, J, and parity are given by Eqs. (2.2) and (2.3).

The formulas here so far are perfectly general. To use them it is only necessary to specify the incoming orbital angular momentum (and hence the function χ) and f_{eff}. For $l=2$, we have

$$\chi(\beta)=(1-3\beta^{-2})+i3\beta^{-1}.\tag{4.18}$$

The methods used in programming these expressions for calculation are outlined in Ref. 15.

f_{eff}

The last step in deriving the D_{13} amplitude is to write explicit expressions from (4.8) for $\mathrm{Re}f_{\mathrm{eff}}$ and $\mathrm{Im}f_{\mathrm{eff}}$ in terms of the parameters f_1, f_2, D, and r_0. For this purpose we define, as in G.L.,

$$y=\kappa r_0,\quad z=Kr_0,\tag{4.19}$$

where κ and K are given by (4.7) and (4.4), respectively.

The lowest mass of the ρ meson occurring in our coupling scheme is $2\,\mu$. Threshold for this is $W=M+2\,\mu$ or, from Eq. (3.5), $T_\pi=[1+\frac{3}{2}(\mu/M)]\mu\approx 170$ MeV. Thus we have, from Eq. (4.8),

(i) For $W<M+2\mu$ ($T_\pi<170$ MeV)

$$\mathrm{Re}f_{\mathrm{eff}}=f_1-\int_{2\mu}^{\infty}dm\rho(m)\left(\frac{1}{y+f_2}\right),\tag{4.20}$$

$$\mathrm{Im}f_{\mathrm{eff}}=0.\tag{4.21}$$

(ii) For $W>M+2\mu$ ($T_\pi>170$ MeV)

$$\begin{aligned}\mathrm{Re}f_{\mathrm{eff}}=f_1&-\int_{2\mu}^{W-M}dm\rho(m)\frac{f_2}{z^2+f_2^2}\\&-\int_{W-M}^{\infty}dm\rho(m)\left(\frac{1}{y+f_2}\right),\end{aligned}\tag{4.22}$$

$$\mathrm{Im}f_{\mathrm{eff}}=-\int_{2\mu}^{W-M}dm\rho(m)\left(\frac{z}{z^2+f_2^2}\right);\tag{4.23}$$

$\rho(m)$ is given by Eq. (4.9).

Again we see that $\mathrm{Im}f_{\mathrm{eff}}\leq 0$. In the Appendix we shall prove that this follows in general from the unitarity of the S matrix, which in turn is equivalent to the Hermiticity of the f matrix.

Care must be taken in evaluating these integrals for $f_2\leq 0$. This choice of f_2 corresponds to a possible ρ-N bound state and will be discussed in greater detail in the conclusions.

To end this section, we shall briefly discuss the behavior of the scattering with f_2. The major contribution to $\mathrm{Re}f_{\mathrm{eff}}$ at energies below threshold for producing the peak of the ρ comes from the second integral in Eq. (4.22). Since $\rho(m)$ is a function peaked at $m^*=5.2\,\mu$ with total area D, we may take the value of the integral as approximately $-D/[y(m^*,W)+f_2]$.

As y and D are positive for $W<M+m^*$, we shall have $\mathrm{Re}f_{\mathrm{eff}}$ decreasing as we approach threshold, at a rate determined by D and f_2. The decrease of $\mathrm{Re}f_{\mathrm{eff}}$ increases the effective attraction in the π-N channel and will bring the phase shift up through $\pi/2$ when it becomes sufficiently negative at a given energy. If $f_2\geq 0$ there is no binding in the ρ-N channel, but the closer f_2 is to zero, the more rapidly we decrease $\mathrm{Re}f_{\mathrm{eff}}$ and hence increase the phase shift. Hence for a narrow resonance we would require f_2 small and positive, for a wide resonance f_2 repulsive (i.e., $f_2\geq 1$).

Fitting the Data

Four parameters are available to us: f_1, f_2, D, and the core radius r_0. We fixed the shape of $\rho(m)$ by letting the ρ-meson mass distribution peak[22] at 720 MeV ($m^*=5.21\,\mu$) and have a full width at half-maximum $=100$ MeV ($\Gamma=0.72\,\mu$).

The long-range diagrams for elastic scattering and production [5(a) and (b), respectively] imply an r_0 in the vicinity of $1-\frac{1}{2}\,\mu^{-1}$. However, as the B.C.M. is based on the assumption that the short range diagrams 5(c) and 5(d) which are of range $\frac{1}{4}$–$\frac{1}{3}\,\mu^{-1}$, play a dominant role in the elastic scattering, we may expect a compromise radius somewhere in the region of $\frac{1}{2}\,\mu^{-1}$. The unscattered wave function for angular momentum l peaks at a distance r determined by $kr\sim l$. At 600 MeV and for $l=2$, we obtain $r\sim 0.6\,\mu^{-1}$. This would make a radius in the vicinity of $\frac{1}{2}\,\mu^{-1}$ favorable.

Rather than f_1 we should like to deal with a quantity analogous to the scattering length in the S-wave case. In general the behavior at zero energy of the phase shift is given by

$$\delta=ak^{2l+1}(k\to 0).\tag{4.24}$$

[22] D. O. Caldwell, E. Bleuler, B. Elsner, L. W. Jones, and B. Zacharov, Phys. Letters **2**, 253 (1962).

For the D_{13} channel this becomes

$$\delta = ak^5. \tag{4.25}$$

Since there is no absorption at zero energy, we may fit the scattering length region with a pure B.C.M.

$$r_0\left(\frac{du}{dr}\right)_{r=r_0,k\to 0} = f_0 u(r_0)_{k\to 0}. \tag{4.26}$$

From Ref. 23 we have the general scattering length formula in terms of f_0 and r_0:

$$\frac{[(2l+1)!!]^2 a}{(2l+1)r_0^{2l+1}} = \frac{(l+1)-f_0}{l+f_0}, \tag{4.27}$$

where channel subscripts are understood on a, f_0, and r_0. [Note that "a" here is defined through Eq. (4.24).] Thus if we call the left-hand expression α, we have

$$f_0 = \frac{(l+1)-l\alpha}{1+\alpha}; \tag{4.28}$$

for $l=2$ (the present case)

$$\alpha = 45a/r_0^5,$$

$$f_0 = \frac{3-2(45a/r_0^5)}{1+(45a/r_0^5)}. \tag{4.29}$$

A graph of f_0 versus a in the d-wave case is shown in Fig. 9.

Then, analogous to Eq. (19) of G.L., we have

$$f_1 = \frac{3-2(45a/r_0^5)}{1+(45a/r_0^5)} + \int_{2\mu}^{\infty} dm\rho(m)\left(\frac{1}{y_0+f_2}\right), \tag{4.30}$$

where y_0 is y evaluated at $k^2=0$.

The method of variation of the parameters was as follows: 3 radii r_0 were attempted; $0.40\,\mu^{-1}$, $0.50\,\mu^{-1}$, and $0.60\,\mu^{-1}$. For each of these radii, $2f_2$'s were tested: 0.25 and 0.50 [attractive but nonbinding S-wave ρ-N force; see discussion on f_2 following Eq. (4.23)]. And for each of these sets (r_0, f_2) several sets of (a,D) were found which gave a resonance at 600 MeV.

As in G.L., all fitting was done by trial and error on the IBM 7090 and 709 computers at MIT. A cutoff of $m=8\,\mu$ was used on all integrals over m with an infinite upper limit. This allows integration over 8 half-widths of the ρ function, and while it entails an error of up to 5% in Ref_{eff}, we keep m^2-W^2 far below M^2 for all values of W considered. [See discussion following Eq. (4.7).] Note, however, that the cutoff is not used because of divergences but as an adequate approximation to a convergent integral. An ordinary Simpson integration routine was used. The interval size $0.1\,\mu$ gave less than 1% variation in a test run when halved, and so was used throughout.

[23] H. Feshbach and E. L. Lomon, Phys. Rev. **102**, 891 (1956).

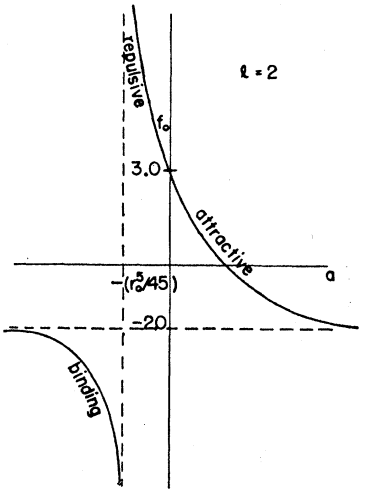

FIG. 9. f_0 versus a for $l=2$: See Eq. (4.29).

V. DISCUSSION OF RESULTS AND CONCLUSIONS

Consistent with theory an $r_0=0.50\,\mu^{-1}$ gave the best fit to both the cross section and the amplitudes. Fig. 1(a) shows the fit to total cross section with $(r_0,f_2)=(0.50, 0.25)$ and two sets of (a,D). In Fig. 1(b) are given the corresponding amplitudes. Figures 2(a), (b) contain similar curves for the case $(r_0,f_2)=(0.50,0.50)$. The parameters for these curves are given in Table I. Finally, Figs. 3 and 4 give the total cross sections for $r_0=0.40$ and 0.60, respectively, with other parameters as given in Table I. The variation of these curves with a change in f_2, a, or D can be deduced from the behavior of Figs. 1 and 2.

Curves A of Figs. 1(a) and 1(b) give the best fit and are good quantitative fits to the elastic and inelastic data from 400 to 700 MeV. The predicted phase shifts at lower energies are also consistent with the data [see Sec. 2(c) below].

We now can draw the following conclusions from these results.

1. General Evaluation

We see that the four variable parameters for the curves in Figs. 1–4 determine amplitudes which in turn give: (a) the position of the resonance, (b) the width,

TABLE I. Parameters for curves in Figs. 1–4.[a]

r_0 (μ^{-1})	f_2	a	D	f_1[b]	Figs.	Set
0.40	0.25	0.00050	2.50	0.78	3	
	0.25	0.00065	5.40	2.74	1	A
		0.00050	6.50	3.51		B
0.50						
	0.50	0.00065	7.00	3.13	2	A
		0.00050	8.50	4.00		B
0.60	0.25	0.00035	11.60	6.09	4	

[a] For all of these, the ρ-meson mass distribution is peaked at 720 MeV, with width 100 MeV.
[b] f_1 is given by Eq. (4.30) in terms of a and D.

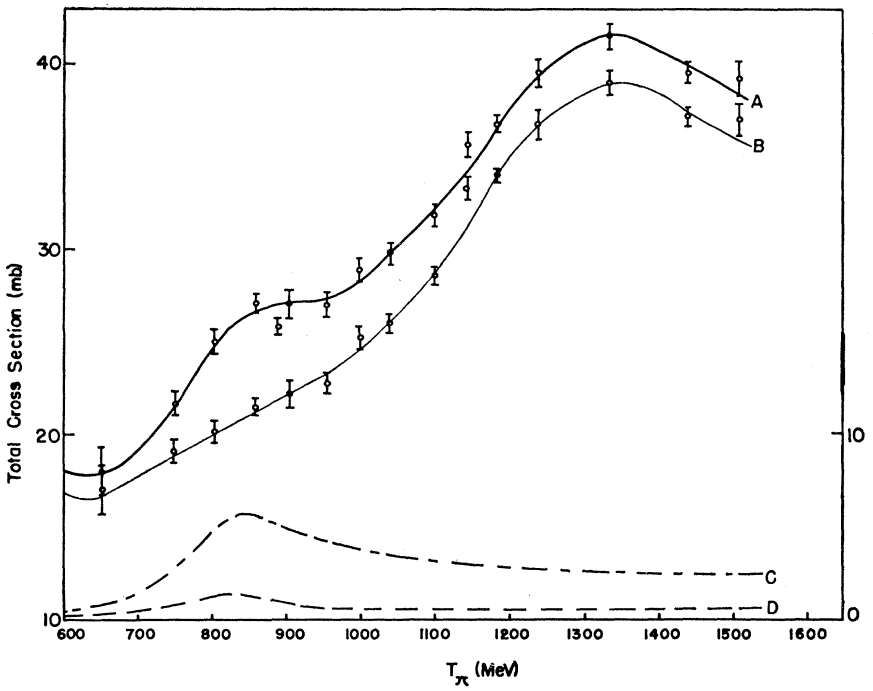

FIG. 10. $T=\frac{3}{2}$ cross section. Curve A: total $\pi^+ + p$ cross section from Ref. 10. Curve C: total D_{33} cross section using parameter of Fig. 1, curve A with the coupling parameter $D=1.80$ in agreement with peripheral model. Curve B: result of subtracting curve C from curve A. Curve D: elastic D_{33} cross section (corresponding to curve C) showing high inelasticity.

(c) the asymmetry of the peak, (d) the inelasticity at resonance; and, (e) the low-energy behavior of δ, consistent with the experimental results.

It is worthwhile to comment at this point on the perhaps unexpected behavior of the inelasticity $1-\eta^2$, which in the Fig. 1(b) has a maximum at $\sim$600 MeV and decreases even as we approach the ρ-peak threshold ($W\sim M+m^*$). A look at Eq. (4.23) shows that $\mathrm{Im}f_{\mathrm{eff}}$ should attain large values near $W\sim M+m^*$. But a careful evaluation of the value of $1-\eta^2$ deduced from Eq. (A11) shows that while $1-\eta^2 \propto |\mathrm{Im}f_{\mathrm{eff}}|$ for $|\mathrm{Im}f_{\mathrm{eff}}| \ll |\mathrm{Re}f_{\mathrm{eff}}|$, it also depends strongly on $\mathrm{Re}f_{\mathrm{eff}}$ through the denominator of Eq. (A11). As a matter of fact, it is characteristic of a resonance that the denominator goes through a minimum at the resonance. Thus, before the resonance $|\mathrm{Im}f_{\mathrm{eff}}|$ and the denominator cooperate to cause a sharp decrease in η, while above the resonance they behave oppositely and η levels off. As in the Breit-Wigner case the resonance in the elastic channel induces a maximum in the inelastic cross section. The model makes no prediction as to the energy of maximum total ρ production in $\pi^{\pm}p$ scattering, since presumably many channels other than the D_{13} are instrumental in ρ production. The analysis of the experimental data into partial waves shows that η does not decrease above resonance in the D_{13} channel, and we reproduce this behavior.

2. Discussion of the Parameters

Let us examine the set of 4 parameters giving the curves A in Fig. 1.

(a) The value of $r_0(=0.50\,\mu^{-1})$ was surmised theoretically before any fitting began, and is consistent with all the considerations in Sec. IV.

(b) The value 0.25 for f_2 suggests that the ρ-N force is strongly attractive in the state $T=\frac{1}{2}$, $J=\frac{3}{2}^-$, but nonbinding. Note that the results are fairly insensitive to f_2 in the range 0.25 to 0.50. The effects of a negative f_2 have not been tested but it is likely to give too narrow a resonance for the correct inelasticity. This case corresponds to the driving of a resonance by the decay of a quasibound state in an inelastic channel[24] and has been proposed previously for the case of the Y_0.* It is being applied now to the case of $\bar{K}$-N scattering by the use of the B.C.M.[25]

(c) The values of a in this case predict the phase shifts at lower energies. For example, at 370 MeV the prediction is for a D_{13} phase shift of 45°. This is in agreement with the analysis of Walker *et al.*[26] Looking now at f_1, which is calculated from a, D, r_0, and f_2, we find it to have a value of around 3. The condition for the phase shift to be zero at any given energy in the π-N channel when $D\to 0$, is that the reduced radial wave function be $krj_2(kr)$, or that $f_1=kr_0[j_2'(kr_0)/j_2(kr_0)]+1$. For $r_0=0.50$ and $k=3.26$ ($T_\pi=600$ MeV), this implies $f_1=2.62$. It is interesting that the curves A have $f_1=2.74$, which corresponds therefore to almost no scattering in the resonance region except that caused

[24] By this we mean that the second channel would have a bound state if uncoupled from the first channel.

[25] E. L. Lomon and C. Yen Liu, Bull. Am. Phys. Soc. 8, 21 (1963). C. Yen Liu, Ph.D. thesis, Massuchusetts Institute of Technology, 1964 (unpublished).

[26] W. D. Walker, J. Davis, and W. D. Shephard, Phys. Rev. 118, 1612 (1960).

by the coupling to the ρ-N channel. If now we look at the D_{33} phase-shift behavior[13] over the first 700 MeV, we find that it is consistent with this hypothesis. As in the S-wave case[7] the experimental difference between the D_{13} and D_{33} states is due to the inelastic channel.

However it is expected that the D_{33} channel is coupled to the S-state ρ-nucleon channel, although more weakly than the D_{13} channel. The one-pion exchange diagram for production of a ρ meson [Fig. 5(a)] leads to a production ratio from the $T=\frac{3}{2}$ state relative to the $T=\frac{1}{2}$ state of $\frac{1}{4}$ [Eq. (3.3)]. As the production [$\propto(1-\eta^2)$] is approximately proportional to our coupling parameter D, reducing D from the $T=\frac{1}{2}$ case by approximately a factor of 4 would correspond to the prediction of the peripheral mechanism. Choosing one of our best $T=\frac{1}{2}$ fits, that of Figs. 1(a), (b), curves A] ($r_0=0.5\,\mu^{-1}$, $f_2=0.25$, $f_1=2.74$, and $D=5.40$) we find that reducing D to 1.80 (keeping *all other parameters fixed*) gives the following excellent results: The D_{33} phase shift is small ($<2°$) and positive, and there is no inelasticity in that channel, up to 550 MeV. This is consistent with the phase-shift analyses available over that energy range. Above 550 MeV, as shown in Fig. 10, the total and inelastic cross sections rise quickly to a maximum (of 5.7 and 4.5 mb, respectively) at 850 MeV. The elastic cross section also attains a small maximum (1.3 mb) at 820 MeV. This explains all the known characteristics of the 850 MeV, $T=\frac{3}{2}$ "shoulder," which has long been attributed to the D_{33} state by Carruthers.[27] We see that subtracting the D_{33} contribution from the experimental total cross section[10] removes the "shoulder." The position and width predicted by our model for this structure adequately corresponds to the experimental knowledge of it. In addition it is known that the "shoulder" is highly inelastic, hardly appearing in elastic data.[9] In our result the peak is only 19% elastic. The large inelasticity is only possible because the peak is not at a resonance. At a resonance Eqs. (2.2) and (2.3) show that a maximum of 50% inelasticity is possible.

3. Comparison with Other Models

Let us compare in more detail our fit to the data with a typical previous attempt. Cook and Lee,[4] using the same inelastic channel, have iterated the peripheral production diagram via the coupled N/D equations. In addition to the parameters describing the ρ meson, they have taken as given the π-N coupling constant and assumed that only the pion exchange is of importance, giving the mass of the exchanged particle. In addition they have replaced the discontinuity across the complex cut (the "strength" of the coupling) with a single pole, using two parameters. With this they do not attempt a fit to all available data, but are successful in obtaining the correct position and a reasonable width. A fit for the D_{33} data would have required a further parameter. When we examine our four parameters, we find that (1) r_0 corresponds to the choice of diagram iterated and to the position of the pole mentioned above; (2) D corresponds to a combination of their Γ (the "strength" parameter) and the π-N coupling constant; (3) f_1 corresponds to a parametrization of all the direct scattering in the elastic channel (which they *assume* to be negligible as a driving force). We have *found* this to be the case [see paragraph (c) of the preceding section]. This parameter allows π-N predictions far from resonance. (4) f_2 corresponds to a parametrization of $\rho N\to\rho N$ scattering. Scattering in this channel is omitted in Ref. 4 and in most other similar approaches because of the lack of knowledge of the analyticity of this amplitude. Because of the small sensitivity of our results to f_2 a similar approach could have been taken in the B.C.M., but having left f_2 in as a free parameter has given us an indication that the $J=\frac{3}{2}$, $T=\frac{1}{2}$ ρ-N S-wave force is attractive, a prediction which may play a role in other experiments.

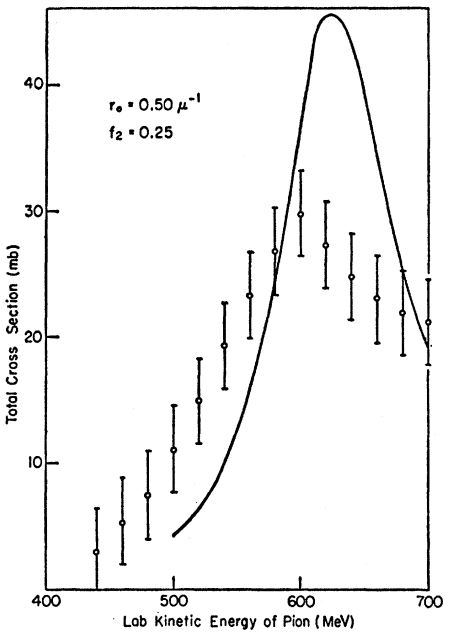

FIG. 11. Total cross section for same r_0, a, D, f_2 of Fig. 1 Set B, but in limit of zero width, to the mass distribution of the ρ meson, still peaked at 720 MeV [i.e., $\rho(m)=D\delta(m-m^*)$].

We have chosen the Cook-Lee paper as an example to elucidate our parametrization. Similar arguments can be given for the other attempts referred to. Lastly, it should be pointed out that the four parameters not only give a good quantitative fit to the D_{13} data, but with a hint from the peripheral diagram, to the D_{33} data as well. This connection of the D_{13} and D_{33} behavior has not been quantitatively established in previous work.[27]

4. The Cook-Lee Mechanism

If we examine the two integrals in Eq. (4.22), we can see that for $T_\pi=600$ MeV ($W-M=4.20\,\mu$), the main

[27] P. Carruthers, Phys. Rev. Letters 4, 303 (1960).

contribution to $\mathrm{Re}f_{\mathrm{eff}}$ comes from the second one, since the peak of $\rho(m)$, lying at $m^*=5.21\,\mu$, is well over $W-M$. Thus in the case presented here unlike in the S-wave case examined in G.L., the production of virtual pions plays the major role in the scattering. Here, as indicated by Cook and Lee, who use the N/D method and approximations for the cut discontinuities, the resonance occurs quite far below threshold. In fact, Fig. 11 shows the results of using the parameters of Fig. 1 (curve B) but reducing the width of the ρ to zero. There is a shift of only 30 MeV in the resonance energy, and of course there is no inelasticity and hence the width is smaller. This shows that it is not the tail of the ρ which drives the resonance as in the Ball-Frazer nanner. Of course, the elegant formalism of Cook and Lee can also handle the effects of real di-pion production, but their choice of ρ-N as the inelastic channel has led them to stress the off-the-mass-shell contributions. The present model supports and extends their interpretation.

We also support their interpretation of the D_{33} "shoulder" as being due to a reduced coupling to the ρ-nucleon channel according to the peripheral diagram. The coupling as they indicate is in this case on the energy shell, as in our S-wave results.

5. Charge Ratios

The coupling assumed for the two pions has considerable consequences in the prediction of charge ratios in the π^-+p production processes. Assuming that the dominant production amplitude has total isospin $T=\frac{1}{2}$, π-$\pi(\rho)$ isospin $t=1$, we deduce (one can use the table in the article by Carruthers[1]) that the cross sections $\sigma(\pi^-+p\to\pi^-+\pi^++n)$, $\sigma(\pi^-+p\to\pi^0+\pi^-+p)$, $\sigma(\pi^-+p\to\pi^0+\pi^0+n)$ are in the ratio 1:2:0. The vanishing of the last cross section follows from the requirement that two π^0's have even angular momentum. Thus we should find negligible double π^0 production at these energies. There is little conclusive data on this prediction. Angular distributions do seem to show isobar production, so that the result of coupling to the third channel $\pi+N\to\pi+N^*$ should be of interest.

6. Importance of Inelasticity

The ability of an inelastic channel to influence scattering way below its threshold[28] (as well as, in the S_{11} case, slightly above threshold) leads to the speculation that the distant singularities are of great importance in using the partial wave dispersion relations; they should be taken care of in a manner which goes beyond the strip approximation. Inelastic unitarity has demonstrated itself as a potent driving force, and its inclusion in a simple, physically meaningful and analytically soluble model has demonstrated its possibilities over a wide energy range. Proposed for future study is to explore the effects on the 900-MeV π-N resonance of producing the ρ meson (here we expect effects analogous to the S_{11} case, since $W-M\sim m^*$) and the effects on the 2-BeV resonance of producing the f^0 meson. Also several analyses[12,29] indicate a rapidly rising P_{11} phase shift in the regions of high inelasticity, and the effects of the different possible inelastic channels on producing this rise may be readily explored by the use of the B.C.M.

[28] For a recent discussion in the context of the Lee model, see H. Chew, Phys. Rev. **132**, 2756 (1963).

7. Use of the B.C.M.

The important mechanism here and in Refs. 6 and 7 is the inelastic coupling. However, the detailed structure of the result has depended on the use of the B.C.M. The quantitative results are an *à posteriori* justification of this choice of model. An *à priori* justification of the B.C.M. has been developed[30] from nonrelativistic and relativistic dynamics. Arguments are presented using reaction theory, the Mandelstam representation and general causality arguments to suggest that this amplitude gives a more meaningful description of strong short range interactions than the standard ones. This eliminates some of the ambiguity of high-momentum contributions which are usually either ignored or cutoff arbitrarily. The long-range predictions of the general B.C.M. are identical to those of "peripheral" or "generalized potential" approaches and can be easily added to a specific B.C.M. model when appropriate.[23]

APPENDIX: THE CONDITION $\mathrm{Im}f_{\mathrm{eff}}\leq 0$ AS A CONSEQUENCE OF UNITARITY

Let the reduced radial wave function be

$$u(r)=\phi^*(r)+S(k)\phi(r), \quad \text{for} \quad r\geq r_0. \tag{A1}$$

$\phi(r)$ is the outgoing solution of the radial wave equation

$$\frac{d^2\phi}{dr^2}+\left(k^2-\frac{l(l+1)}{r^2}-V(r)\right)\phi(r)=0, \quad r\geq r_0, \tag{A2}$$

where $V(r)$, the potential tail, is in general a real function of r and k.

Multiplying (A2) by ϕ^* and (A2)* by ϕ, and then subtracting we obtain

$$\frac{d}{dr}\left[\phi^*\frac{d\phi}{dr}-\phi\frac{d\phi^*}{dr}\right]=0, \tag{A3}$$

i.e., the Wronskian

$$W=\phi^*\frac{d\phi}{dr}-\phi\frac{d\phi^*}{dr} \tag{A4}$$

is independent of r. Thus we can calculate it by substituting for $\phi(r)$ in (A4) its asymptotic form, which is $(-i)^{l+1}\,e^{ikr}$ (except for a Coulomb potential). Doing this we obtain

$$W=2ik. \tag{A5}$$

[29] William M. Layson, Nuovo Cimento **27**, 724 (1963).

[30] H. Feshbach and E. Lomon, Ann. Phys. (N. Y.) (to be published).

Thus

$$\mathrm{Im}\left[\phi^*\frac{d\phi}{d(kr)}\right]=1, \quad \text{for all } r. \tag{A6}$$

Now, from Eq. (4.14) we write $S=\eta e^{2i\delta}$ in terms of $f_{\text{eff}}\equiv f_r+if_i$

$$S=-\left(\frac{f_{\text{eff}}\phi^*-\beta\phi^{*\prime}}{f_{\text{eff}}\phi-\beta\phi^{\prime}}\right), \tag{A7}$$

where the prime denotes differentiation with respect to kr, $\beta\equiv kr_0$ and ϕ, ϕ', ϕ^*, $\phi^{*\prime}$ are evaluated at $kr=\beta$.

$$\therefore S=\frac{A^*+i\phi^*f_i}{A+i\phi f_i}, \tag{A8}$$

where $A\equiv f_r\phi-\beta\phi'$.

$$\therefore |S|^2=\frac{|A|^2+f_i^2|\phi|^2-2f_i\,\mathrm{Im}A\phi^*}{|A|^2+f_i^2|\phi|^2+2f_i\,\mathrm{Im}A\phi^*}. \tag{A9}$$

But

$$A\phi^*=f_r|\phi|^2-\beta\phi'\phi^*.$$

$$\therefore \mathrm{Im}A\phi^*=-\beta\,\mathrm{Im}\phi^*\frac{d\phi}{d(kr_0)}$$

$$=-\beta \quad [\text{from (A4)}]. \tag{A10}$$

Thus, from (A9) and (A10),

$$|S|^2=\frac{|A|^2+f_i^2|\phi|^2+2\beta f_i}{|A|^2+f_i^2|\phi|^2-2\beta f_i}$$

$$\leqslant 1, \text{ if and only if, } \mathrm{Im}f_{\text{eff}}\leq 0; \tag{A11}$$

we know that $|S|^2\leq 1$, if and only if, f is Hermitian. Thus, f is Hermitian, if and only if,

$$\mathrm{Im}f_{\text{eff}}\leq 0. \tag{A12}$$

PHYSICAL REVIEW VOLUME 134, NUMBER 3B 11 MAY 1964

Departures from the Eightfold Way: Theory of Strong Interaction Symmetry Breakdown*

SIDNEY COLEMAN

AND

S. L. GLASHOW†

Lyman Laboratory of Physics, Harvard University, Cambridge, Massachusetts

(Received 14 November 1963)

We consider the three kinds of departure from exact unitary symmetry: medium-strong interactions which leave only isospin and hypercharge as good symmetries, electromagnetism, and weak interactions. We postulate the existence of an octet of scalar mesons that give the possibility of symmetry-breaking tadpole diagrams. Our fundamental dynamical assumption—that symmetry-violating processes are dominated by symmetry-breaking tadpole diagrams—gives an immediate explanation of the success of two empirical laws: the Gell-Mann–Okubo mass formulas and the nonleptonic $\Delta I=\frac{1}{2}$ rules. Moreover, including tadpole diagrams and some other electromagnetic corrections, we calculate the six electromagnetic mass splittings of mesons and baryons in terms of a single unknown parameter correctly to within 0.5 MeV.

I. INTRODUCTION

WE assume that the fundamental interactions of elementary particles fall into the following classes, arranged in order of diminishing strength (we omit gravity):

1. Very-strong interactions, invariant under the transformations of "the eightfold way"—the symmetry scheme of Gell-Mann[1] and Ne'eman,[2] based on the group SU(3).

2. Medium-strong symmetry-breaking interactions, invariant under only the isospin-hypercharge subgroup of SU(3). Whether these interactions are introduced at the beginning, or whether they arise by some kind of spontaneous symmetry breakdown is immaterial to our discussion.

3. Electromagnetism.

4. Weak interactions.

* Supported in part by the U. S. Office of Naval Research, Contract NONR-3656(09), and by the U. S. Air Force Office of Scientific Research, under contract number A.F. 49(638)589.

† Alfred P. Sloan Foundation Fellow. On leave from the Physics Department of the University of California at Berkeley, California.

[1] M. Gell-Mann, California Institute of Technology Synchrotron Report CTSL-20, 1961 (unpublished); Phys. Rev. **125**, 1067 (1962).

[2] Y. Ne'eman, Nucl. Phys. **26**, 222 (1961).